TURBULENCE-COMBUSTION INTERACTION IN DIRECT INJECTION DIESEL ENGINE

by

Mohamed BENCHERIF [a,c*], ***Mohand TAZEROUT*** [b], ***and Abdelkrim LIAZID*** [c]

[a] University of Science and Technology in Oran, Oran, Algeria
[b] Ecole des Mines de Nantes, DSEE, France
[c] LTE Laboratory – ENSET, Oran, Algeria

Original scientific paper
DOI: 10.2298/TSCI121210084B

The experimental measures of chemical species and turbulence intensity during the closed part of the engine combustion cycle are today unattainable exactly. This paper deals with numerical investigations of an experimental direct injection Diesel engine and a commercial turbocharged heavy duty direct injection one. Simulations are carried out with the KIVA3v2 code using the re-normalized group (k-ε) model. A reduced mechanism for n-heptane was adopted for predicting auto-ignition and combustion processes. From the calibrated code based on experimental in-cylinder pressures, the study focuses on the turbulence parameters and combustion species evolution in the attempt to improve understanding of turbulence-chemistry interaction during the engine cycle. The turbulent kinetic energy and its dissipation rate are taken as representative parameters of turbulence. The results indicate that chemistry reactions of fuel oxidation during the auto-ignition delay improve the turbulence levels. The peak position of turbulent kinetic energy coincides systematically with the auto-ignition timing. This position seems to be governed by the viscous effects generated by the high pressure level reached at the auto-ignition timing. The hot regime flame decreases rapidly the turbulence intensity successively by the viscous effects during the fast premixed combustion and heat transfer during other periods. It is showed that instable species such as CO are due to deficiency of local mixture preparation during the strong decrease of turbulence energy. Also, an attempt to build an innovative relationship between self-ignition and maximum turbulence level is proposed. This work justifies the suggestion to determine otherwise the self-ignition timing.

Key words: *Diesel engine, turbulence, combustion, chemistry reduced mechanism, simulation, KIVA3v2*

Introduction

The complex interaction of physical and chemical processes of combustion in direct injection (DI) diesel engine determines its overall performance and emission characteristics. Using experimental investigations to get the turbulence intensity and the average evolution of chemical species during the closed part of the engine cycle is not easy to achieve due to technical challenges and very expensive cost [1, 2]. This is why the numerical tools as computational fluid dynamics (CFD) codes constitute an important and useful alternative to get some reasonable comprehension of the studied phenomena. Currently, great help seems to be offered by the use of the CFD tools in order to guide researchers to better understanding and predicting compres-

* Corresponding author; e-mail: m_bencherif@yahoo.com

sion ignition engine performances and emission levels. Indeed, an enhanced understanding of the processes taking place in the combustion chamber and the link between parameters in order to explore new solutions reduces the cost and improves the efficiency [3, 4]. KIVA-3v code developed at Los Alamos National laboratory is one of the most widely used packages for three dimensional engine simulation tools using an arbitrary Lagrangian-Eulerian methodology [5-8]. KIVA-3v released version using reduced or detailed chemistry and new turbulence-chemistry interaction model was achieved at Chalmers University of Technology in Gothenburg, Sweden [9]. The detailed mechanism integrating the n-heptane oxidation chemistry with kinetics of aromatics formation has been incorporated into the KIVA-3v2. Calculations performed by the released version of KIVA-3v code give the advantage to have a close composition to real exhaust gases which extends capabilities of the code to predict fuel spray auto-ignition and combustion [9-11]. It has been shown that models with detailed and reduced chemistry of aliphatic components such as n-heptane can be used to simulate Diesel engines according to their cetane number (~56) which is similar to the cetane number of conventional Diesel fuel. It has been reported that the difference in combustion models seems not critical when physical properties of the model fuel as well as the n-heptane are represented by properties of real Diesel oil [9, 11]. This paper uses a turbulence-chemistry interaction model [9] based on a reduced chemistry of n-heptane in the attempt to carry out analysis between the evolution of turbulent parameters (k, ε) and those related to chemistry during the closed part of the engine cycle. It's evident that at the end of the compression stroke, the swirl and tumble eddies are weakened leading to a more homogeneous turbulent flow which is determinant for the next periods of the engine cycle process. The aim of this work is to improve understanding of turbulence-combustion interaction.

Experimental set-up

Two Diesel engines are experienced in this study. The first one is the experimental Lister-Petter DI Diesel engine. It is a single cylinder connected to an automatic controlled eddy current dynamometer. The second engine is a commercial turbocharged heavy duty direct injection Diesel engine called MKDIR. In-cylinder pressure, top dead centre (TDC) and injection pressure signals are acquired with a rapid data acquisition system (AVL-Indiwin) and stored on computer. The data from 100 consecutive cycles are recorded and processed with specific automatic vehicle localization (AVL) company software. All thermodynamic parameters (pressures, temperatures, flow rates) of air and fuel flows and mechanical parameters (rotational speed, torque) are measured using locally developed acquisition software. The main engines specifications are given in tabs. 1 and 2.

Table 1. Specifications of the Lister-Petter engine

Parameter	Specification
Engine type	Lister-Petter type S1
No. of cylinders	Single cylinder
Rated power	5.4 kW at 1800 rpm
Cylinder bore	95.25 mm
Upper bowl diameter	45.00 mm
Stroke length	88.5 mm
Compression ratio	18:1

Table 2. Specifications of the MKDIR engine

Parameter	Specification
No. of cylinders	06
Cylinder bore	120 mm
Stroke length	145 mm
Connecting rod length	227 mm
Compression ratio	17
Maximum torque	158 daNm (ISO) at 1200 rpm
Rated power	264 kW at 2400 rpm

The experimental Lister-Petter engine is always operated at its rated speed of 1500 rpm. However, the MKDIR engine is operated at rotational speed of 1400 rpm. Partial and full loads are selected such as the engines operate on a wide range. The engines are mechanically and thermally stabilized before taking all measurements. The injection timing is optimized and set respectively at 18° CA bTDC for the Lister-Petter engine and at 8° CA bTDC for the MKDIR one.

In-cylinder numerical investigation

CFD investigations have been performed in the attempt to evaluate the combustion-turbulence interaction in the engine cylinder using the KIVA3v-2 code in order to achieve the fuel spray and combustion processes during the closed part of the engine cycle.

Governing equations

The CFD code solves the following governing equations.

– Continuity equations for species m:

$$\frac{\partial \rho_m}{\partial t} + \nabla(\rho_m u) = \nabla\left[\rho D \nabla\left(\frac{\rho_m}{\rho}\right)\right] + f_m + \dot{\rho}_m^s \delta_{m1} \tag{1}$$

where ρ_m is the mass density of species m and ρ – the total mass density, u – the velocity, $\dot{\rho}_m^c$ – the source term due to the chemistry, $\dot{\rho}^s$ – the source term due to the spray, and δ – the Dirac delta function. By summing the previous equation over all species we obtain the total fluid density equation:

$$\frac{\partial \rho}{\partial t} | \nabla(u\rho) = \dot{\rho}^s \tag{2}$$

– Since mass is conserved in chemical reactions the fluid momentum equation for the fluid mixture is:

$$\frac{\partial(\rho u)}{\partial t} + \nabla(\rho u u) = -\nabla p + \nabla\sigma + F^s + \rho g - \frac{2}{3}\nabla(\rho k) \tag{3}$$

where p is the fluid pressure, F^s – the rate of momentum gain per unit volume due to the spray.

– Finally the internal energy conservation is:

$$\frac{\partial(\rho I)}{\partial t} + \nabla(\rho u I) = -p\nabla u - \nabla\vec{\mathrm{J}} + \rho\varepsilon + \dot{Q}^c + Q^s \tag{4}$$

where I is the specific internal energy, exclusive of chemical energy. The heat flux vector $\vec{\mathrm{J}}$ is the sum of contributions due to heat conduction and enthalpy diffusion terms. $\dot{Q}^s$ and $\dot{Q}^c$ are terms due to spray interactions and chemical heat, respectively. The KIVA3v2 code solves the previous equations taking account of the dysphasic aspect of evaporating fuel sprays and three dimensional turbulent fluid dynamics for a compressible multi-component, reactive mixtures in the engine cylinder with arbitrary shaped piston geometries [10]. The famous break-up model associated with fuel parcels collision, drag, coalescence and evaporation is used to reproduce the spray atomization of fuel effect in the combustion chamber [12].

Turbulence-combustion model

The source term, $\dot{\rho}_m^c$, in the species transport equation is a function of the combustion zone parameters, it is dependent on variables, not on a grid level, but on a sub-grid level. Hence, using only grid level information "straight on" is, in most cases, not appropriate as the combus-

tion region structure is not resolved. Because of this, correlating the sub-grid conditions with grid level conditions is a necessity, since the grid level conditions are the only information available. Golovitchev *et al.* [13] have performed one approach to how to treat this problem. This approach leads to the turbulence-chemistry interaction model adopted in this study. This model operates with a multi-step reaction mechanism [9]. It is based on the generalization of the partially stirred reactor (PaSR) model taking account for the effect of mixture imperfections on chemical reaction rates. This model is detailed in the references [13, 14] and can be summarized by the following equation expressing the chemical source term on a sub-grid level:

$$\dot{\rho}_m(c') = \kappa \dot{\rho}_m(c) \tag{5}$$

where

$$\kappa = \frac{\tau_c}{\tau_c + \tau_{mix}} \tag{6}$$

The effect of the chemical concentration c' is replaced with the rate multiplier κ. The parameter c is the averaged concentration in the cell. It is important to observe that when $\tau_{mix} \to 0$, the model reduces to the quasi-laminar approach with $c \equiv c'$ in the reaction rate terms. Inversely, in the limit of fast chemistry ($\tau_c \ll \tau_{mix}$) the model reproduces the Magnussen eddy dissipation rate. The characteristic time τ_{mix} exerts the main influence on the exchange process between the fresh, un-reacting mixture and the burned gases. There is a wide range of scales in turbulent flows, from the largest eddies down to the molecular level, and to account for all these different scales using only one characteristic value is of course a great simplification. Hence, from the RNG k-ε turbulence model, two definitions are proposed by Golovitchev [14]. The first one is similar to the Taylor time scale $\tau_{mix} \approx (c_\mu/R_{et})^{1/2} k/\varepsilon$ where $c_\mu = 0.09$ and the second one expressed as $\tau_{mix} \approx \Delta^{2/3}\varepsilon^{-1/3}$ is used when smallest eddies are enlarged to be resolved by the computer grid. The parameter Δ is the minimal scale resolved on the grid. The second definition grants for the model a quality of the sub-grid scale (SGS) approach. The reduced mechanism of n-heptane used in this study is with 42 equations with the following species C_7H_{16}, O_2, N_2, O, H, OH, HO_2, H_2O_2, H_2O, H_2, CO, CO_2. As it is impractical to consider neat n-heptane as a real fuel for Diesel engines, then we carried out the engine simulations using the "hybrid" mode, in which fuel physical properties correspond to real diesel oil, but with a combustion mechanism corresponding to n-heptane chemistry with a corrected fuel/oxidizer stoichiometry. This approach of the engine simulations is validated by Golovitchev *et al.* [13-15]. The turbulence model used is therefore the RNG (k-ε) model [9, 10, 13].

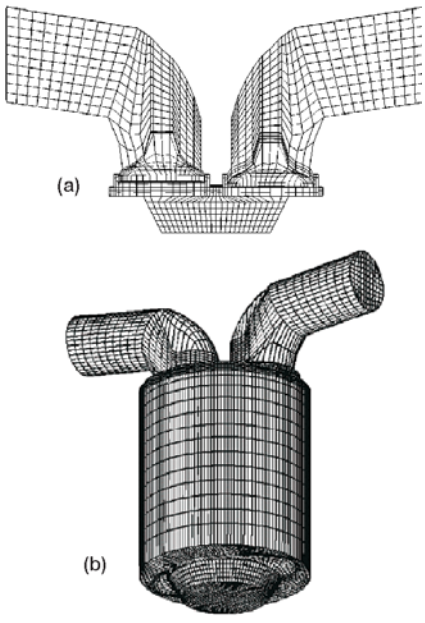

Figure 1. Grid meshes for the computational domain; (a) Lister-Petter engine, (b) MKDIR engine

Meshing domain

A 3-D grid with 180 degree sector configuration has been used. The mesh was created such as the boundary was flagged and adjusted to have the real geometry (bore, stroke, *etc*.,…). The mesh resolution used for the Lister-Petter engine is 40 × 17 × 12 cells

in the squish region and 24 × 12 × 6 cells in the bowl region. The entire calculation domain is formed by 23924 cells with 24013 vertices. The mesh resolution used for the MKDIR engine is the same than that of the Lister-Petter one but with a different geometry. Figure 1 represents the generated grid meshes corresponding, respectively, to the Lister-Petter engine when the piston is at TDC position and the MKDIR engine when the piston is at the bottom dead center (BDC).

Boundary conditions

Initial conditions required for launching calculations are flow pressure and temperature at the intake, exhaust and in-cylinder, the turbulent kinetic energy and its dissipation rate, the length scale and the swirl ratio. The initial pressure and temperature values are set from measured pressure at the intake, exhaust and in-cylinder. The length scale is taking as the engine bore diameter. However, turbulent kinetic energy, swirl ratio, and boundary temperatures are fixed according to the values proposed by literature and the software developers [5-8]. The initial conditions in the combustion chamber for each engine are recapitulated in tab. 3.

Table 3. Initial conditions for the studied engines

Lister-Petter engine at CA = 137° bTDC		MKDIR engine at CA = 138° bTDC	
400 K	Gas temperature	650 K	Gas temperature
1.16 MPa	Gas pressure	1.6 MPa	Gas pressure
0.16 cm^2/s^2	Initial turbulent kinetic energy	0.16 cm^2/s^2	Initial turbulent kinetic energy
0.12 cm	Initial length scale	0.12 cm	Initial length scale
0.5	Initial swirl ratio	0.5	Initial swirl ratio

Initial and boundary conditions must be specified for each equation. Three types of wall boundary are chosen. Only the first one (piston head) is set as translate and other boundaries were set as stationary and smooth. Law of the wall is used for gas temperature and velocity. Injection velocities have been specified using experimental injection pressure profiles.

Code validation

For the Lister-Petter engine, the CFD code validation is based on the comparison between experimental and numerical results of in-cylinder pressure for partial and full load at the engine speed of 1500 rpm. Partial load is selected at 60%. This procedure is sufficient in the case of the Diesel engine due to its regular and reproducible cycle, contrary to the spark ignition engines where the flame development and subsequent propagation vary cycle by cycle [1]. Figures 2(a), 2(b), and 2(c) represent the evolution of predicted and measured in-cylinder pressures during the engine cycle for each applied load. Good agreement is shown between measured and computed in-cylinder pressures. Hence, the CFD code gives a prediction of in-cylinder pressure during compression, before the fuel injection and during combustion process. The small discrepancies observed at the end of the piston expansion stroke and near the pressure peaks can be attributed to modeling imperfections of the in-cylinder heat transfer process. We can say for all cases that there is an acceptable agreement between computed and measured in-cylinder pressure. Figure 3 shows the predicted heat-release rates for various applied loads using the in-cylinder pressure data, heat transfer and crevice effects [1]. For the MKDIR engine the code validation is also achieved with the same accuracy as shown at the next section.

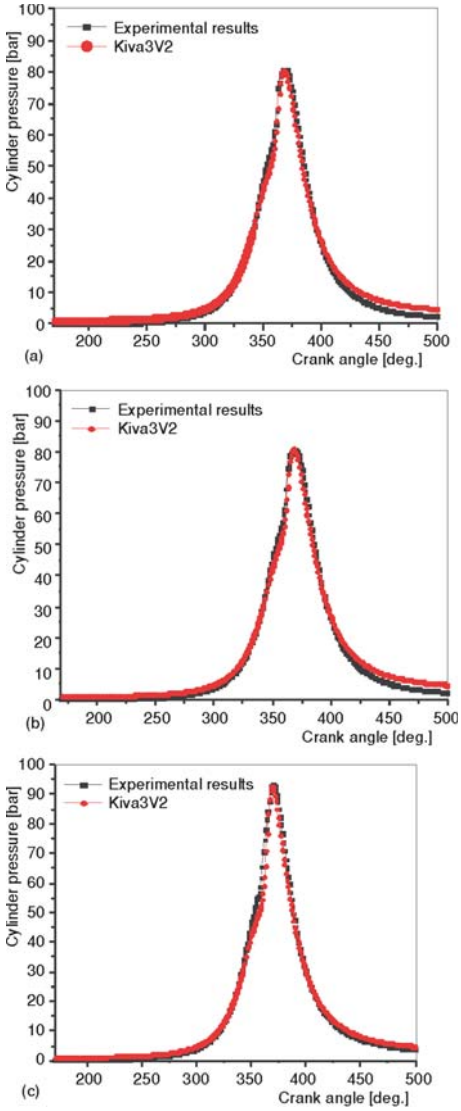

Figure 2. Engine in-cylinder pressure; (a) N = 1500 rpm, 20% load, (b) N = 1500 rpm, 60% load, (c) N = 1500 rpm, 100% load

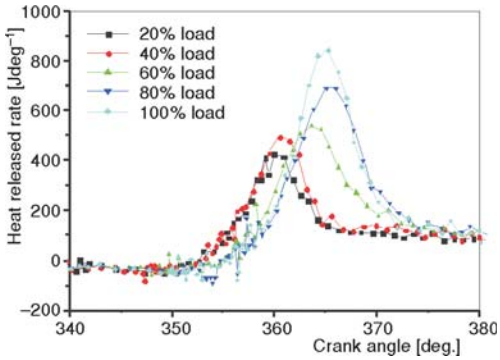

Figure 3. Predicted heat released rates at N = 1500 rpm (Lister-Petter engine)

Results and discussions

The results related to the Lister-Petter engine are firstly presented and followed by the MKDIR ones.

Turbulence spectra

In order to reduce the paper length, figs. 4 and 5 show the spectra of turbulent kinetic energy (TKE) and its dissipation rate only for 60% of engine load. Similarly trends are observed for the other loads (20% and 100%). At each one, these spectra are plotted both for fired and unfired engine cycle. One must specify that for unfired cycle the combustion routine was deactivated but with maintaining the injection of fuel. Hence, some observations can be pointed.

– Both for TKE and its dissipation rate, the peak magnitude is higher for the fired cycle than the unfired one at each engine load. Therefore chemical oxidation of fuel improves the level of turbulence. Based on the analysis of figs. 4 and 5, it can be pointed that the TKE peak position is located at 10° CA before the peak position of the corresponding heat-released rate. This means just at the self-ignition timing. This observation is reported in tab. 4.
– Both for fired and unfired cycle, the position of TKE peak is the same at each engine load. This remains true for the dissipation rate. This result indicates that the position of turbulence peak is independent of chemistry and corresponds systematically to the self-ignition timing (start of the hot regime flame). Therefore, the TKE peak position is governed only by the viscous phenomena generated by the pressure at self-ignition timing.

From these observations it can be confirmed that the maximum TKE magnitude results from in-cylinder flows from intake and compression and shear during the first half-period of in-

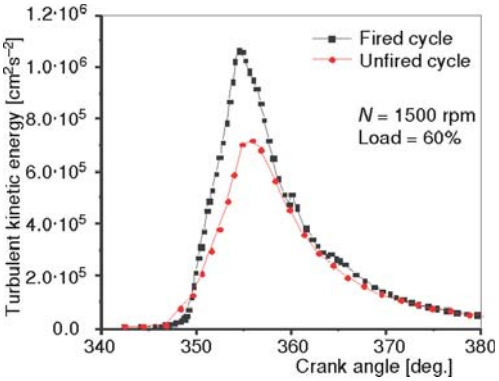

Figure 4. Turbulent kinetic energy evolution Lister-Petter engine

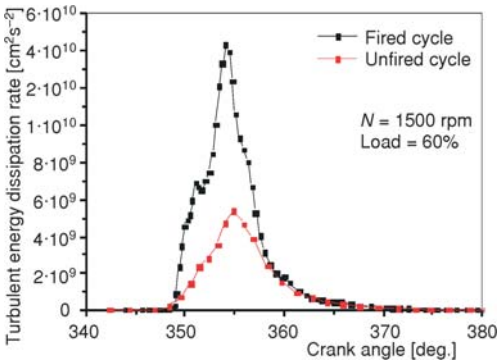

Figure 5. Turbulent kinetic energy dissipation rate evolution Lister-Petter engine

jection event. For the fired cycle the chemical oxidation of fuel improves the TKE levels during the second half-period of ignition delay. Thus, in the compression ignition engine, it can be deduced that the viscous phenomena generated by the pressure at self-ignition timing are the main responsible of the TKE peak position, independently of chemistry. From the TKE peak position, the heat released rate (HRR) of fast premixed combustion boost up rapidly the in-cylinder pressure which promotes the viscous effects leading to the rapid drop of the turbulence intensity. This tendency continues during the expansion stroke due to the temperature decrease. Close to the TDC, it can be seen in fig. 4 a small jump of the TKE at partial load probably due to the squish phenomenon resulting from radial in-cylinder flows.

Table 4. Turbulence peak positions and auto-ignition timing (Lister-Petter engine)

Load	Peak position of TKE	Peak position of HRR	Auto-ignition timing
20%	350° CA	360° CA	350° CA
60%	354° CA	364° CA	354° CA
100%	357° CA	366° CA	357° CA

According to the relationship between the average turbulent intensity and the mean piston speed proposed in the reference [1], the maximum TKE can be estimated according the following equation:

$$\frac{\sqrt{k_{\max}}}{\bar{S}_P} = 243\mathrm{e}^{0.01(T/T_{\max})} \tag{7}$$

Hence, another way to estimate the self-ignition delay can be expressed directly according to the maximum TKE as:

$$\tau_{\mathrm{id}} = 0.065\frac{k_{\max}}{(k_{\max})_{\mathrm{full-load}}} \tag{8}$$

The previous relations represent an attempt to estimate the timing of hot regime combustion starting, avoiding the determination of auto-ignition delay according to thermodynamic (temperature and pressure) and chemical (activation energy) parameters. It is important to specify that these results represent a first step for further works with a large class of direct injection engines.

Chemical species

The evolution of CO_2, H_2O, CO, and OH components are similar for each considered load, so we choice for illustration the case corresponding of 60% engine load on figs. 6 and 7. Figure 8 shows the evolution of the O and H components for the arbitrary case of 100% engine load. From fig. 6 it can be observed that the production of CO_2 and H_2O species start at the self-ignition timing and accelerate rapidly during the premixed period of combustion where the mixture temperature increases strongly leading to the hot flame regime. This is well known for the combustion of hydrocarbons as reported in specialized literature [2]. During the other combustion periods, the CO_2 and H_2O concentrations continue to increase slowly as a logarithmic form. The CO and OH species begin to appear from the end of the premixed combustion period where a default of local oxygen occurs due to the TKE depletion as mentioned above. Hence, the global quality of combustion is affected. However, the fuel diminution during the late combustion period, starting around 375° CA, reduces the CO production. Figure 8 illustrates the evolution of the chemical species H and O. It can be noticed that at the end of the fast non-premixed combustion 370° CA, the remaining oxygen does not realize a good local mixture due to the strong decrease of TKE. However, during the late combustion period started close to 375° CA, these species decrease due to the temperature drop. Furthermore, the curve shapes of O and H species are similar to those of the CO with a high magnitude near the end of the fast premixed period of combustion. From this moment the depletion of O and H species enhances the OH species which is a good indicator of the combustion process quality. This species rises at the late combustion period which indicates the kinetic chemistry behavior.

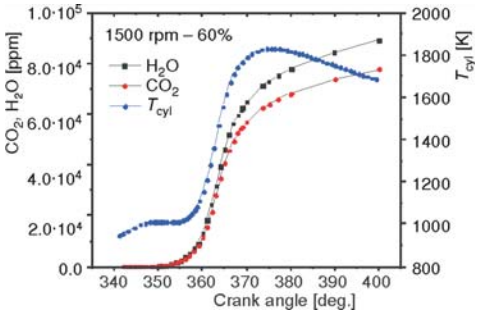

Figure 6. Predicted temperature of H_2O and CO_2 species

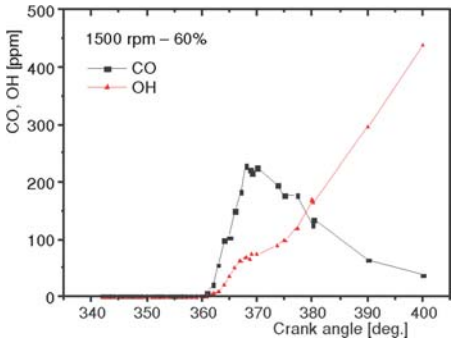

Figure 7. Predicted of CO and OH species

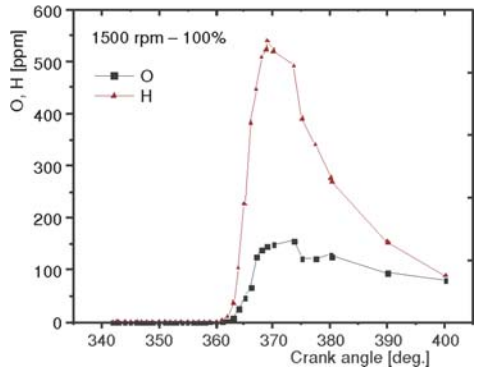

Figure 8. Predicted of O and H species

MKDIR engine

Let us now consider the MKDIR Diesel engine. The experimental tests achieved on this engine are carried out for several regimes and loads. For the illustration need in this study, the arbitrarily selected operating case of 1400 rpm at 60% of engine load is considered. Figure 9 shows the code calibration based on the in-cyl-

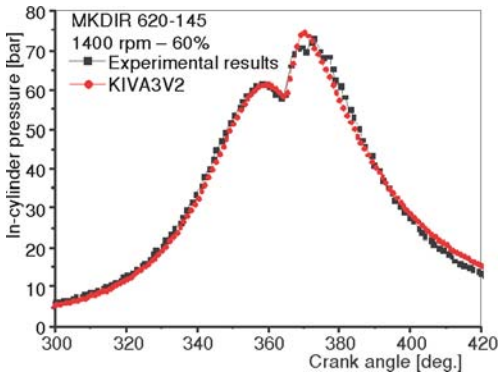

Figure 9. Engine in-cylinder pressure; N = 1400 rpm, 60% (MKDIR engine)

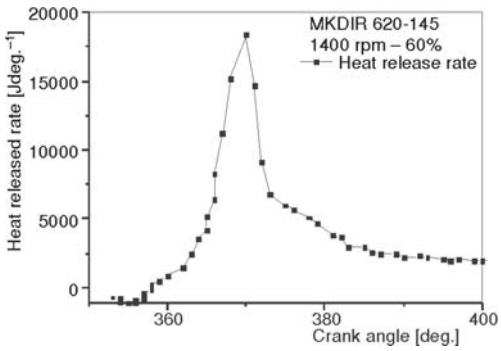

Figure 10. Predicted heat released rates at N = 1400 rpm (MKDIR engine)

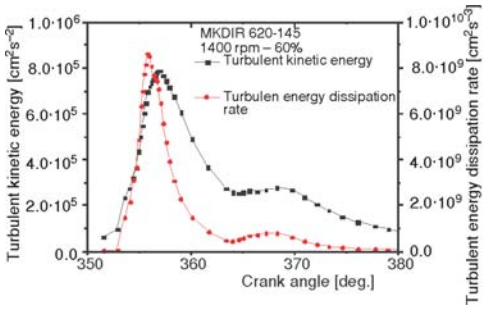

Figure 11. Turbulent kinetic energy and its dissipation rate evolution (MKDIR engine)

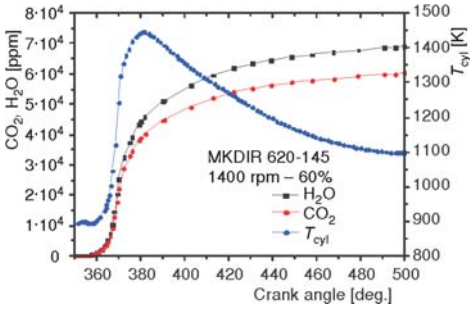

Figure 12. Predicted temperature and H_2O, CO_2 species (MKDIR engine)

inder pressure. The injection timing starts at 8° CA bTDC. Figure 10 shows that the premixed combustion period starts at 4° CA bTDC and finishes at 10° CA aTDC. The CA of starting combustion corresponds to the TKE peak as deduced from figs. 10 and 11. Before TDC, the combustion starts moderately due to the small amount of premixed gases. It really accelerates from 3° CA aTDC with a small increase of TKE that fades rapidly due to viscous effects even if the spray momentum rate increases generating a strong acceleration of the premixed combustion as observed after the TDC. The CO_2 and H_2O species appear during the premixed combustion period leading to a rapid increase of the in-cylinder temperature as shown in fig. 12. The CO and OH species shown in fig. 13 begin to appear at the end of the premixed combustion period due to the slow level of TKE leading to a deficiency of local mixtures. The same situation is observed for O and H species, fig. 14. Conse-

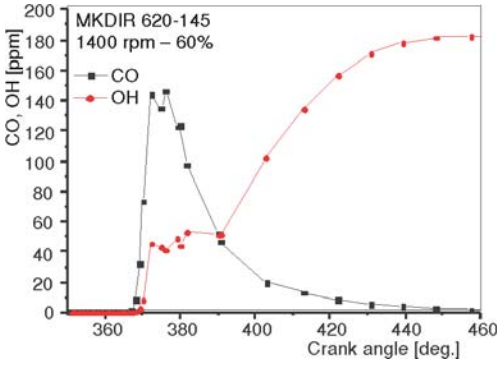

Figure 13. Predicted CO, OH species (MKDIR engine)

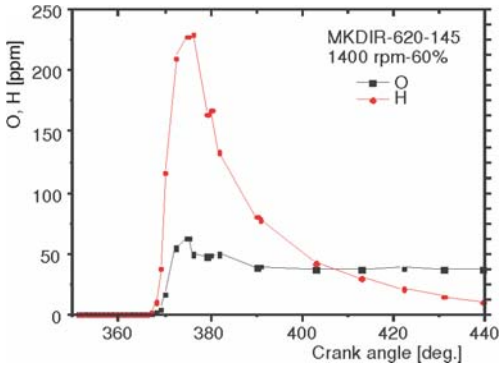

Figure 14. Predicted O, H species (MKDIR engine)

quently, the turbulence-combustion mechanism of this engine is similar than the Lister-Petter engine.

All the previous results help us to understand that the in-cylinder interaction of turbulence-combustion process during a cycle of a DI Diesel engine can be globally explained by the following observations.

The turbulence peak position is essentially governed by the viscous effects due to the strong gradients of pressure at the end of combustion stroke. The first step of the combustion (*e. g.* the premixed combustion period) is greatly influenced by the achieved magnitude of the turbulence energy level generated during the ignition delay period and essentially caused by the in-cylinder flows and fuel sprays. After this period (*e. g.* during the non-premixed phase) the combustion process is governed by the kinetic chemical process.

Conclusions

This work contributes to identify clearly how the interaction between turbulence and combustion occurs during a cycle of a DI Diesel engine. The complexity and the high experimental devices technology and cost levels required for such investigations have oriented us to a numerical investigation. The computer code KIVA3v2 has been used in order to carry out and analyze the turbulence-combustion interactions for the experimental DI Lister-Petter engine. The observations of the obtained results are confirmed by those of a commercial turbocharged heavy duty DI Diesel engine. The reduced mechanism used in this study consists on the n-heptane with a global reaction supplemented by a species set involving in 42 reactions. The RNG (k-ε) model was used for modelling turbulence. The results reported in this paper illustrate manifestly the premixed, fast non premixed and diffusion periods of the combustion process. From the discussions of these results it can be concluded that the viscous phenomena generated by the pressure level at auto-ignition timing determine the peak positions of TKE and its dissipation rate regardless the chemical reactions of fuel oxidation. Hence, the TKE peak position corresponds systematically to the auto-ignition timing indicating the start of the hot regime flame which drops drastically the turbulence levels. A relationship between self-ignition and maximum turbulence level is proposed. It constitutes a first step to more research investigations in this field. The evolution of CO_2 and H_2O species during the diffusion period of combustion is hardly influenced by the turbulence drop. However, the CO, O, and H species appear during the fast non premixed period of combustion process. This is due to deficiency of mixture preparation. This is attributed to drop of turbulence resulting from the growth of viscous effects followed by the temperature depletion effects. Hence, the combustion process is governed by the chemical kinetic.

Nomenclature

c – grid level concentration species
c' – sub-grid scale concentration species
F^s – rate momentum gain per unit volume due to the spray
f_m – chemical source term
g – specific body force, [ms^{-2}]
I – specific internal energy, [Jkg^{-1}]
J – heat flux vector, [Wm^{-2}]
k – turbulent kinetic energy [m^{2}s^{-2}]
p – pressure, [Nm^{-2}]

Q^c – chemical source term
Q^s – spray source term
S_P – mean piston speed, [ms^{-1}]
T – torque, [Nm]
T_{cyl} – cylinder temperature, [K]

Greek symbols

α – diffusion coefficient
ε – turbulent dissipation rate, [m^{2}s^{-3}]
ρ_m – density of chemical species m, [kgm^{-3}]
ρ_m^s – mass density source term for species m due to spray, [kgm^{-3}]
ρ_m^c – mass density source term for species m due to chemistry, [kgm^{-3}]
τ_c – chemical time
τ_{id} – self-ignition time
t_{mix} – characteristic time for turbulence

Acronyms

aTDC – after top dead centre
bTDC – before top dead centre
CA – crank angle
CFD – computational fluid dynamic
DI – direct injection
rpm – revolution per minute
RNG – re-normalized group
TDC – top dead centre
TKE – turbulent kinetic energy

References

[1] Heywood, J. B., *Internal Combustion Engine Fundamentals*, Mc Graw-Hill. Inc., New York, USA, 1983
[2] Günter, P. M., *et al*., *Simulating Combustion, Simulation of Combustion and Pollutant Formation for Engine-Development*, Springer-Verlag Berlin, Heidelberg, Germany, 2006
[3] Bencherif, M., *et al*., Pollution Duality in Turbocharged Heavy Duty Diesel Engine, *Int. J. Vehicle Design, 50* (2009), 1-4, pp. 182-195
[4] Jafarmadar, S., *et al*., Modeling the Effect of Spray/Wall Impingement on Combustion Process and Emission of DI Diesel Engine, *Thermal Science, 13* (2009), 3, pp. 23-34
[5] Amsden, A. A., *et al*., KIVA-II: A Computer Program for Chemically Reactive Flows with Sprays, Technical report, Los Alamos National Laboratory, LA-11560-MS, Los Alamos, N. Mex., USA, 1989
[6] Amsden, A. A., KIVA-3, A KIVA Program with Block-Structured Mesh for Complex Geometries, Technical Report, Los Alamos National Laboratory, LA-12503-MS, Los Alamos, N. Mex. USA, 1993
[7] Amsden, A. A., KIVA-3V, A Block-structured KIVA Program for Engines with Vertical or Canted Valves, Technical Report, Los Alamos National Laboratory, LA-13313-MS, Los Alamos, N. Mex., USA, 1997
[8] Amsden, A. A., KIVA-3V, Released 2, Improvements to Kiva-3v, Technical Report, Los Alamos National Laboratory, LA-13608-MS, Los Alamos, N. Mex., USA,1999
[9] Golovitchev, V. I., *et al*., 3-D Diesel Spray Simulations Using a New Detailed Chemistry Turbulent Combustion Model. SAE, paper 00FL-447, 2000
[10] Jarnicki, R., *et al*., Numerical Simulation of Spray Formation, Ignition and Combustion in a Diesel Engine, Using Complex Chemistry Approach, Los Alamos, N. Mex., USA, *International Combustion Engines, 7* (2000), 1-2, pp. 247-257
[11] Golovitchev, V. I., *et al*., Towards Universal EDC-Based Combustion Model for Compression Ignited Engine Simulations. JSEA, 2003-0181, SAE paper 2003-01-1849
[12] Reitz, R. D., Rutland, C. J., Development and Testing of Diesel Engine CFD Models, *Progress in Energy and Combustion Science, 21* (1995), pp. 173-196
[13] Golovitchev, V. I., *et al*., 3-D Diesel Spray Simulations Using a New Detailed Chemistry Turbulent Combustion Model, SAE, paper 2000-01-1891, 2000
[14] Golovitchev, V. I., Revising "Old" Good Models: Detailed Chemistry Spray Combustion Modeling Based on Eddy Dissipation Concept, *Proceedings*, 5th International Conference Internal Combustion Engine, 2001, Capri, Naples, Italy
[15] Golovitchev, V. I., *et al*., Numerical Evaluation of Soot Formation Control at Diesel -Like Conditions by Reducing Fuel Injection Timing; SAE, paper 1999-01-3552, 1999

Paper submitted: December 10, 2012
Paper revised: May 18, 2013
Paper accepted: June 26, 2013